Automated Detection of Choroid Boundary and Vessels in Optical Coherence Tomography Images

N. Srinath, A. Patil, V. Kiran Kumar, S. Jana,
Indian Institute of Technology Hyderabad
Andhra Pradesh, India-502205
{ee10b028,ee10b030,ee11p012,jana}@iith.ac.in

J. Chhablani, A. Richhariya,
L.V. Prasad Eye Institute, Hyderabad
Andhra Pradesh, India-500034
jay.chhablani@gmail.com,ashutosh@lvpei.org

***Abstract*— Structural changes in the choroid, a layer located between the retina and sclera, could indicate various vision impairments. Consequently, ophthalmologists inspect optical coherence tomography (OCT) scans of the posterior section of the eye towards making diagnosis. With a view to assist diagnosis, we propose an automated technique for segmentation of the choroid layer. Specifically, we detect the upper and lower boundaries of the choroid using structural similarity and adaptive Hessian analysis. Subsequently, we detect choroid vessels within those boundaries using a level set method. Experimental results are presented using spectral domain (SD) OCT images.**

I. Introduction

Various vision impairments are indicated by reduction in thickness and depletion of blood vessels in the choroid, a layer located between the retina and the sclera in the posterior part of the eye [1], [2]. Ophthalmologists ascertain choroid health by visually inspecting optical coherence tomography (OCT) images of the posterior visual section. With a view to assisting them, we present an automated technique for segmentation of the choroid layer, and detection of choroid vessels in OCT images.

As shown in Fig. 1a, a typical OCT image depicts the en-face image (left), and the cross-section at the dotted line on the en-face image (right). The cross-section further depicts retina, choroid, and sclera, respectively, from top to bottom. The upper boundary of choroid is sharply demarcated by the bright retinal pigment epithelium (RPE), the deepest sublayer of retina. In contrast, the lower boundary with the sclera is less dramatic, and will demand most of our attention. Specifically, we shall use structural similarity (homogeneity) of sclera to separate it from choroid, and refine the result by adaptively thresholding the Hessian matrix at each point.

Based on choroid boundaries, thus detected, next we detect choroid vessels using level set method. The level set is used for iterative minimization of an energy function involving the estimated mutual information between the rival classes to achieve the segmentation. Upon convergence, the zero level contour of the level set function is taken as the segmentation boundary.

In view of the deep medical implications, unsurprisingly, choroid segmentation has been widely studied. For instance, a technique involving multiscale Hessian matrix analysis and region growing has recently been reported [3]. Another method makes use of 3D edge filtering and projection of probability cones [4]. Graph-based multistage segmentation has also been attempted [5]. A connected components algorithm has been applied on denoised and enhanced images as well [6]. Unfortunately, despite certain attempts [7], consensus on a standardized evaluation of algorithmic results in terms of medical relevance is yet to evolve. In the meantime, it is worthwhile to explore the problem from various perspectives. In this vein, we employ structural similarity, Hessian analysis and level set method to attempt a solution.

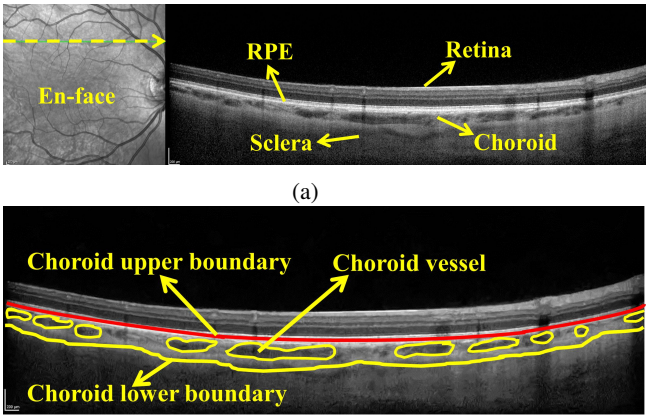

Fig. 1: (a) Typical OCT image (courtesy Dr. William R Freeman, University of California, San Diego, La Jolla, CA), and (b) Choroid upper boundary, choroid lower boundary and choroid vessels indicated manually.

We demonstrate our algorithm using spectral domain OCT (SD-OCT) images. The detected boundary hugs the outer envelope of choroidal vessels. Variation of choroid thickness is also plotted. Finally, choroid vessels are detected, and visually authenticated by experts. The organization of rest he paper is as follows. The problem is formulated in Sec. II, and mathematical preliminary is presented in Sec. III, while Sec. IV describes the proposed methodology. Experimental results are given in Sec. V. Finally, Sec. VI concludes the paper.

II. Problem Formulation

With a view to assisting ophthalmologists visualize the choroid layer and vessels, we aim at automatizing the detection of the choroid boundary and the segmentation of choroidal blood vessels. For the ease of execution, we divide

978-1-4244-7929-0/14/$26.00 ©2014 IEEE

the problem into two distinct steps: (i) detection of choroid boundary, and (ii) detection of choroidal vessels using the detected choroid boundary. To this end, we shall leverage the fact that choroid and sclera layers have different statistical properties as evidenced by visual dissimilarity. Hence, we formulate the problem in terms of perceptually quality metric and Hessian matrix analysis for detecting choroid boundary. On the other hand, unique statistical properties of choroidal vessel are then exploited to segment those vessels using a level set problem. Interestingly, a natural choice for the energy functional turns out to be the mutual information.

III. Mathematical Preliminary

In this section, we introduce a few mathematical notions.

A. Structural Similarity Index

The structural similarity (SSIM) index for two windows A and B of equal size is given by [8]

$$SSIM(A,B) = \frac{(2\mu_A\mu_B + c_1)(2\sigma_{AB} + c_2)}{(2\mu_A^2\mu_B^2 + c_1)(\sigma_A^2 + \sigma_B^2 + c_2)},$$

where μ_A and μ_B denote the mean, and σ_A^2 and σ_B^2 denote the variance of windows A and B, respectively, σ_{AB} is the covariance, and c_1 and c_2 indicate small constants, chosen to avoid certain technical difficulties. Later we shall use SSIM of sclera to separate it from choroid.

B. Eigenvalue analysis of the Hessian matrix

Let J(q) denote the intensity at image location $q = (x, y)$. The second order approximation of J(q) around $q = q_0$ is given by [9]

$$J(q) = J(q_0) + (q - q_0)^T \nabla J_0 + 0.5(q - q_0)^T \nabla^2 J_0 (q - q_0),$$

where ∇J_0 denotes the gradient vector and $\nabla^2 J_0$ denotes Hessian matrix at q_0. Note that the Hessian matrix of image $J(q)$ is computed as

$$H = \nabla^2 J(q) = \begin{bmatrix} J_{xx}(q) & J_{xy}(q) \\ J_{yx}(q) & J_{yy}(q) \end{bmatrix}, \tag{1}$$

where the entries are the second order partial derivatives. Supposing λ_1 and λ_2 ($\lambda_1 < \lambda_2$) are eigenvalues of H, then for points in tubular dark regions, λ_1 is small and λ_2 is large [10]. We shall use this property towards detecting choroid vessels.

C. Level set method for image segmentation

For a scaler function $v(q)$ and region R whose boundary is denoted by the curve $\overrightarrow{C}$, define the energy functional $E(\overrightarrow{C}(t))$ as

$$E(\overrightarrow{C}(t)) = \int_{R(\overrightarrow{C}(t))} v(q)\ dq. \tag{2}$$

The curve evolution that minimizes $E(\overrightarrow{C}(t))$ in (2) is given by the gradient flow equation [11]

$$\frac{\partial \overrightarrow{C}}{\partial t} = -v\overrightarrow{N}, \tag{3}$$

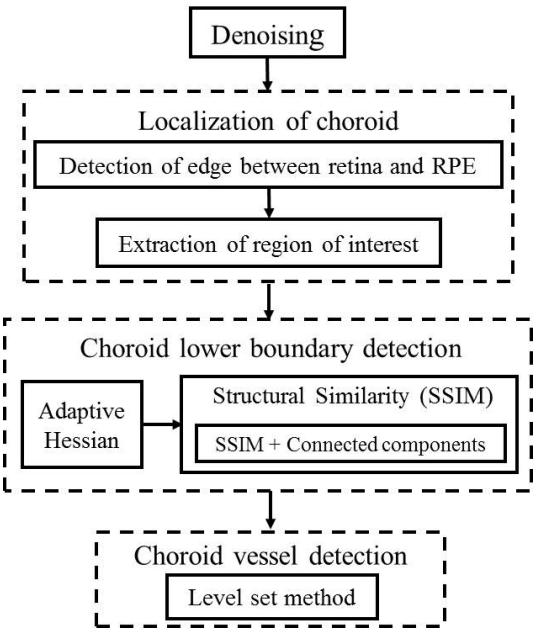

Fig. 2: Flow chart of proposed methology

where $\overrightarrow{N}$ denotes the inward normal. Notice that $v(q)$ acts as a velocity field. Defining a level set function ϕ such that $\overrightarrow{C}(t)$ becomes its zero level contour, (3) maps to level set evolution [12]

$$\frac{\partial \phi}{\partial t} = -v|\nabla\phi|. \tag{4}$$

One now needs to choose energy functional $E(\overrightarrow{C}(t))$, and hence level set function ϕ, for the binary segmentation of image Γ. Of course, one desires $\overrightarrow{C}(t)$ to converge to the decision boundary. Denote by $\hat{R}_1$ the region inside $\overrightarrow{C}(t)$, and by $\hat{R}_0$ that outside. Equivalently, define the label function $L_{\overrightarrow{C}}(q) = i$, if point $q \in \hat{R}_i$. Denoting by Q a location random variable taking values q in Γ, it can be shown that the mutual information $I(J(Q); L_{\overrightarrow{C}}(Q))$ is maximum when label values for all pixel locations are correct [13], which thus provides us the energy functional. Practically, one uses

$$E(\overrightarrow{C}) = -|\Gamma|\hat{I}(J(Q); L_{\overrightarrow{C}}(Q)) + \alpha \oint_{\overrightarrow{C}} ds, \tag{5}$$

where $\hat{I}(J(Q); L_{\overrightarrow{C}}(Q))$ denotes estimated mutual information, $\oint_{\overrightarrow{C}} ds$ the length of the curve, α a scalar weight, and $|\Gamma|$ the total number of pixels in the image. The last distance regularization term in (5) helps in practical implementation [14].

From (5), we derive the level set evolution equation as

$$\begin{aligned}\frac{\partial \phi}{\partial t} = \Bigg[\log\left(\frac{\hat{p}_1(J(\overrightarrow{C}))}{\hat{p}_0(J(\overrightarrow{C}))}\right) + \frac{1}{|\hat{R}_1|}\int_{\hat{R}_1} \frac{K(J(q) - J(\overrightarrow{C}))}{\hat{p}_1(J(q))} dq \\ - \frac{1}{|\hat{R}_0|}\int_{\hat{R}_0} \frac{K(J(q) - J(\overrightarrow{C}))}{\hat{p}_0(J(q))} dq \Bigg] |\nabla\phi| \\ - \alpha\left(\vec{\nabla}\cdot(\nabla\phi)\right)/|\nabla\phi|,\end{aligned} \tag{6}$$

where probability densities $\hat{p}_1$ and $\hat{p}_1$ of respective classes are estimated using Gaussian kernel [15].

IV. Proposed Methodology

In this section, we propose a hierarchical method for detecting choroid boundary and choroid vessels as depicted in Fig. 2. Specifically, we employ SSIM and Hessain analysis for the former and a level set method for the latter.

A. Denoising and Localization of Choroid

To begin with, OCT images are denoised using the block-matching and 3D filtering (BM3D) algorithm which takes advantage of underlying sparsity [16]. We localize the choroid region below retina by exploiting the brightness of the RPE region. Specifically, we make use of edge detection, dilation and connected components [17]. Further, we take a region of interest (ROI) of uniform thickness below RPE to accurately locate the choroid. We flatten the ROI by removing the inherent curvature for ease of processing.

B. Choroid Lower Boundary Detection

Observing that the sclera and the choroid layers have very different structures, we take a small window from the sclera as the template, and use the SSIM index to match the remainder of the sclera. What remains left out is then declared as the choroid. Specifically, SSIM is particularly low near the lower edges of large choroid vessels. Note that some outliers are expected, and removed using connected components alogorithm. While our SSIM technique is generally effective, it does leave out certain areas of the choroid. This gap is filled based on eignvalues of the Hessian matrix by detecting dark tubular structures as mentioned earlier.

C. Choroid Vessel Detection

Once both the upper and the lower boundaries of the choroid are detected, the level set method is used to segment choroid vessels. The level set function is confined within these boundaries, and initialized with a suitable step function. Referring to Sec. III-C, now we label choroid vessels as region R_1 and rest of the choroid as R_0. As noted, we iteratively maximize certain mutual information that leads to the desired decision boundary upon convergence. Next we turn to presenting experimental results.

V. Experimental Results

In this section, we illustrate effectiveness of the proposed methodology. Our data-set consists of OCT images of the posterior part of the eye taken with 30 μm separation. The images are obtained using Heidelberg Retina Angiograph (HRA - Spectralis, Heidelberg Engineering, Dossenheim, Germany). We first detect the choroid boundaries and then segment choroid vessels in 2D.

Fig. 3b shows the denoised version of image shown in Fig. 3a using BM3D [16]. Subsequently, Fig.3c shows the RPE upper boundary detected to localize the region of interest and Fig.3d shows the extracted region of interest below RPE. Notice that ROI is straightened for easier processing. Fig. 3e shows the initial output after applying SSIM. There are some outliers dectected in sclera, which are removed by connected components and the corresponding result is shown in Fig. 3f. Subsequently, we choose the envelope to get final SSIM output (see Fig. 3g). Notice that, Fig. 3g shows gaps in the choroid boundary. The missing portion of the boundary is recovered using an adaptive Hessian technique. Fig. 3h shows the final choroid boundary after

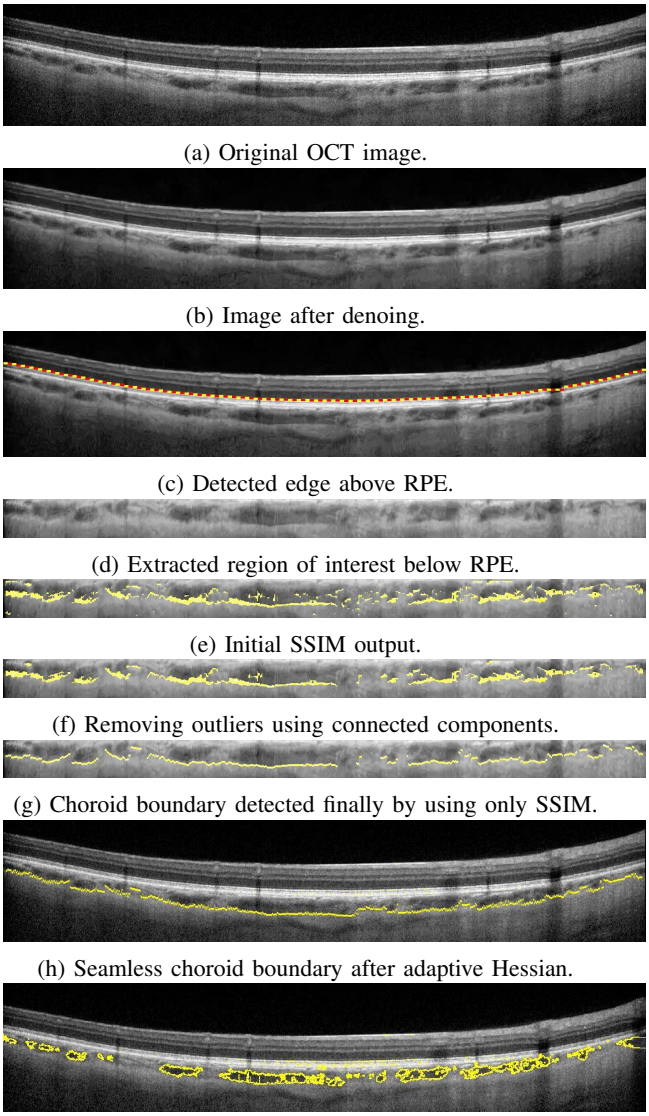

(a) Original OCT image.

(b) Image after denoing.

(c) Detected edge above RPE.

(d) Extracted region of interest below RPE.

(e) Initial SSIM output.

(f) Removing outliers using connected components.

(g) Choroid boundary detected finally by using only SSIM.

(h) Seamless choroid boundary after adaptive Hessian.

(i) Choroid vessels segmented using level set method

Fig. 3: Denoising, localization of choroid, choroid boundary and vessel detection.

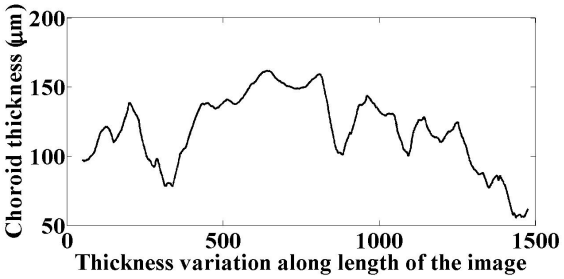

Fig. 4: Choroid thickness variation plot

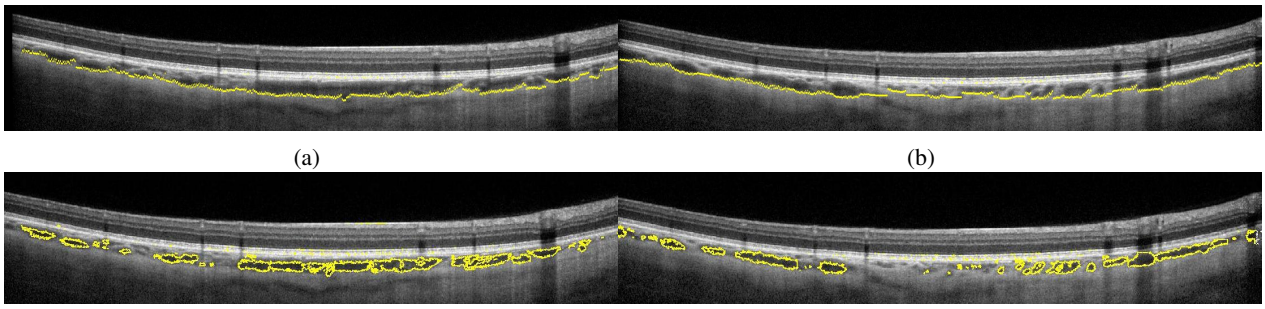

(a) (b)

(c) (d)

Fig. 5: (a) and (b): Detected choroid boundary of different OCT images; (c) and (d): Large and medium sized choroidal vessels detected in corresponding images (a) and (b).

combing adaptive Hessian output with of the SSIM output. Level set requires proper initialization to detect only the vessels present in choroid, therefore the boundary is used as limits for initialization for the choroid vessel segmentation. Fig. 3i shows the final segmentation. It can be observed that large and medium sized vessels are detected with reasonable accuracy.

Fig. 4 gives thickness plot of the choroid layer of image given in Fig. 3a. This provides the variation of the thickness along the length of the OCT image. Finally, we present repeatability of our algorithm by applying it to different OCT images. Fig. 5 shows the results for detection of choroid boundary and choroid vessels for two different OCT images apart from that of shown in Fig. 3a.

VI. Discussion

In this paper, we proposed a novel approach for choroid boundary detection using SSIM and adaptive Hessian analysis. Further, we proposed a level set technique for choroid vessel segmentation. Experimental results for both the methods are presented. We note that the choroid boundary marked by experts generally is a smooth curve below choroid vessels, while the boundary detected using proposed method hugs those vessels. To detect the expected boundary, further work and more advanced techniques are needed. At the same time, 2D segmentation of choroid vessels aid in diagnosis only to a limited extent. It does not provide complete sense of choroidal vasculature and corresponding thickness variation in space, for which one should be able visualize choroid vessels in 3D. In future, we shall extend our results to 3D by stacking the segmented 2D choroid vessels with appropriate geometric alignment, and visualize in true 3D on a lightfield display.

References

[1] D. L. Nickla and J. Wallman, "The multifunctional choroid," *Progress in retinal and eye research*, vol. 29, no. 2, pp. 144–168, 2010.

[2] L. Wu, and N. Alpizar-Alvarez, "Choroidal imaging by spectral domain-optical coherence tomography," —em Taiwan Journal of Ophthalmology, vol. 3, no. 1, pp. 3–13, 2013.

[3] L. Zhang, K. Lee, M. Niemeijer, R. F. Mullins, M. Sonka, and M. D. Abramoff, "Automated segmentation of the choroid from clinical sd-oct, *Investigative ophthalmology & visual science*, vol. 53, no. 12, pp. 7510–7519, 2012.

[4] V. Kajić , E. Marieh, G. Carl, F. K. Martin, H. Joachim, O. Richu, B. Susanne, G. F. James, and D. Wolfgang, "Automated three-dimensional choroidal vessel segmentation of 3D 1060 nm OCT retinal data," *Biomedical optics express*, vol. 4, no. 1, pp. 134–150, 2013.

[5] Z. Hu, X. Wu, Y. Ouyang, Y. Ouyang, and S. R. Sadda, "Semiautomated segmentation of the choroid in spectral-domain optical coherence tomography volume scans," *Investigative ophthalmology & visual science*, vol. 54, no. 3, pp. 1722–1729, 2013.

[6] N. R. Mahajan, R. C. R. Donapati, S. S. Channappayya, S. Vanjari, A. Richhariya, and J. Chhablani, "An automated algorithm for blood vessel count and area measurement in 2-D choroidal scan images," *Engineering in Medicine and Biology Conference (EMBC)*, pp. 3355–3358, Osaka, Japan, 2013.

[7] L. R. Dice, "Measures of the amount of ecologic association between species," *Ecology*, vol. 26, no. 3, pp. 297–302, 1945.

[8] Z. Wang, A. C. Bovik, H. R. Sheikh and E. P. Simoncelli, "Image quality assessment: From error visibility to structural similarity," *IEEE Transactions on Image Processing*, vol. 13, no. 4, pp. 600–612, April 2004.

[9] Y. Sato, S. Nakajima, N. Shiraga, H. Atsumi, S. Yoshida, T. Koller, G. Gerig, and R. Kikinis, "Three-dimensional multi-scale line filter for segmentation and visualization of curvilinear structures in medical images," *Medical image analysis*, vol. 2, no. 2, pp. 143–168, 1998.

[10] A. F. Frangi,W. J. Niessen, K. L. Vincken, and M. A. Viergever, "Multiscale vessel enhancement filtering," *Medical Image Computing and Computer-Assisted Interventation (MICCAI)*, pp. 130–137, Cambridge MA, USA, 1998.

[11] S. C. Zhu, and A. Yuille, "Region competition: Unifying snakes, region growing, and bayes/mdl for multiband image segmentation," *IEEE Transactions on Pattern Analysis and Machine Intelligence*, vol. 18, no. 9, pp. 884–900, 1996.

[12] S. Osher, and J. A. Sethian, "Fronts propagating with curvature-dependent speed: algorithms based on hamilton-jacobi formulations," *Journal of computational physics*, vol. 79, no. 1, pp. 12–49, 1988.

[13] J. Kim, J. W. Fisher, A. Yezzi, M. etin, and A. S. Willsky, "A non-parametric statistical method for image segmentation using information theory and curve evolution," *IEEE Transactions on Image Processing*, vol. 14, no. 10, pp. 1486–1502, 2005.

[14] C. Li, C. Xu, C. Gui, and M. D. Fox, "Distance regularized level set evolution and its application to image segmentation," *IEEE Transactions on Image Processing*, vol. 19, no. 12, pp. 3243–3254, 2010.

[15] E. Parzen, "On estimation of a probability density function and mode," *Annals of mathematical statistics*, vol. 33, no. 3, pp. 1065–1076, 1962.

[16] K. Dabov, A. Foi, V. Katkovnik, and K. Egiazarian, "Image denoising by sparse 3-D transform-domain collaborative filtering,"*IEEE Transactions on Image Processing*, vol. 16, no. 8 , pp. 2080–2095, 2007.

[17] V. K. Kumar, T. R. Chandra, S. Jana, A. Richhariya, and J. Chhablani, "3D Visualization and Mapping of Choroid Thickness based on Optical Coherence Tomography: A Step-by-Step Geometric Approach," *International Conference on 3D Imaging (IC3D)*, pp. 1–8, Liége, Belgium, 2013.